Journal of Biomolecular NMR, 8 (1996) 391–403
ESCOM

J-Bio NMR 393

Elucidation of the origin of multiple conformations of the human α3-chain type VI collagen C-terminal Kunitz domain: The reorientation of the Trp^{21} ring

Morten Dahl Sørensen[a], Søren M. Kristensen[a], Søren Bjørn[b], Kjeld Norris[b], Ole Olsen[b] and Jens J. Led[a,*]

[a]*Department of Chemistry, University of Copenhagen, The H.C. Ørsted Institute, Universitetsparken 5, DK-2100 Copenhagen Ø, Denmark*
[b]*Health Care Discovery, Novo Nordisk A/S, Novo Allé, DK-2880 Bagsværd, Denmark*

Received 1 August 1996
Accepted 12 August 1996

Keywords: Collagen; Kunitz domain; Multiple conformations; Exchange rate

Summary

The human α3-chain type VI collagen C-terminal Kunitz domain fragment (α3(VI)) has been studied by two-dimensional ^1H-^1H and ^1H-^{13}C NMR spectroscopy at 303 K. It is shown that the secondary structure of the protein is strikingly similar to that of BPTI, and that a number of unusual H^{α} chemical shifts, which are highly conserved in Kunitz-domain proteins, are also observed for α3(VI). Furthermore, a series of exchange cross peaks observed in ^1H-^1H spectra shows that a large number of protons in the central β-sheet exist in two different chemical environments, corresponding to two unequally populated conformations that are slowly exchanging on the NMR time scale. Several protons, including $Ser^{47(53)}$ H^{α}, $Arg^{32(38)}$ $H^{\gamma 1}$ and $H^{\gamma 2}$, and $Gln^{48(54)}$ $H^{\beta 2}$, all located in the vicinity of the $Trp^{21(27)}$ ring in the crystal structure of α3(VI) [Arnoux, B. et al. (1995) *J. Mol. Biol.*, **246**, 609–617], have very different chemical shifts in the two conformations, the most affected being $Gln^{48(54)}$ $H^{\beta 2}$ ($\Delta\delta = 1.53$ ppm), which is placed directly above the $Trp^{21(27)}$ ring in the crystal structure of α3(VI). It is concluded that the origin of the multiple conformations of the central β-sheet is a reorientation of the $Trp^{21(27)}$ ring. From the intensities of corresponding signals in the two conformations, the population of the minor conformation was found to be $6.4 \pm 0.2\%$ of that of the major conformation, while a rate constant $k_M = 1.01 \pm 0.05$ s^{-1} for the major to minor interconversion was obtained from a series of NOESY spectra with different mixing times. In addition, it is shown that $Cys^{14(20)}$-$Cys^{38(44)}$ disulfide bond isomerization, previously observed in BPTI [Otting, G. et al. (1993) *Biochemistry*, **32**, 3571–3582], is also likely to occur in α3(VI).

Introduction

Human type VI collagen is composed of three polypeptide chains, α1, α2 and α3, which form a heterotrimeric molecule with short triple-helical and large globular domains at both ends. The α3-chain was shown by Chu et al. (1990) to possess a sequence in the most C-terminal domain, C5, of approximately 60 residues which is highly similar to sequences of serine protease inhibitors. Similar sequences have also been found in other large proteins, e.g. in a precursor protein of Alzheimer β-amyloid protein (Kitaguchi et al., 1988; Ponte et al., 1988; Tanzi et al., 1988). Common for these large proteins is an approximately 60-residue sequence with a high homology to the bovine pancreatic trypsin inhibitor (BPTI), one of the most thoroughly studied proteins.

Recently, the NMR solution structure of the 76-residue complete C5 domain (Zweckstetter et al., 1996) and the X-ray crystal structure of the 7–64 fragment (Arnoux et al., 1995) were published. For the C5 domain it was shown that the solution structure consists of a well-defined 55-residue core (residues 8–62) and 7 N-terminal

*To whom correspondence should be addressed.

Supplementary material: Tables (4 pages) containing the ^1H and ^{13}C chemical shifts of α3(VI) are available upon request from the authors.

and 12 C-terminal disordered residues. The 55-residue core of the C5 domain and the crystal structure of the 7–64 fragment were both found to retain the characteristic fold of the Kunitz-type inhibitor family. However, despite this agreement between the overall folds obtained by X-ray and NMR, Zweckstetter et al. found that the complete C5 domain exists in exchanging multiple conformations, and that there are three patches of residues that have multiple conformations; one in the central β-sheet, one in the loop around the Cys^{20}-Cys^{44} disulfide bond, and one in the vicinity of the Cys^{11}-Cys^{61} disulfide bond. In contrast, no evidence for the presence of multiple conformations of the 7–64 fragment was found in the crystallographic data.

In the light of the inextricable link between protein function and atomic motion (see e.g. Wodak et al. (1987) and Williams (1989) for reviews), it is important to determine whether the disagreement between the NMR and X-ray studies is a consequence of the difference in the sequences of the two proteins, or if it is due to the differences in states and methods. Furthermore, precise knowledge of the origin of the multiple conformations is indispensable for the assessment of their influence on protein activity.

Here we present an independent NMR study of the 7–64 fragment of the C5 domain. It is shown that multiple conformations do indeed exist for the 7–64 fragment in solution, and that the origin of the multiple conformations in the central β-sheet is a reorientation of the $Trp^{21(27)}$ ring. The rate of this reorientation is $1.01 \pm 0.05\ s^{-1}$ at 303 K, as determined by 2D NMR.

In the following, the 7–64 fragment is referred to as α3(VI). Throughout this paper, sequence numbers of α3(VI) will start with residue 1 to maintain direct comparison with the well-known BPTI. Sequence numbers in parentheses refer to the corresponding sequence number in the complete C5 domain.

Materials and Methods

Sample preparation

α3(VI) was prepared using the procedure outlined by Arnoux et al. (1995). The pH of the NMR samples was between 2.8 and 3.0 (direct meter reading), and the concentration of the protein varied from 2 to 5 mM.

NMR experiments

The ^1H-^1H homonuclear and ^1H-^{13}C heteronuclear spectra were recorded on a BRUKER AM500 spectrometer, operating at 500 MHz for protons. All spectra were recorded with sequential quadrature detection in the t_2 dimension (Redfield and Kunz, 1975) and time-proportional phase incrementation (TPPI) in the t_1 dimension (Drobny et al., 1979; Bodenhausen et al., 1980; Marion and Wüthrich, 1983), allowing the spectra to be represented in the phase-sensitive mode. Water suppression was achieved using a DANTE pulse scheme (Bodenhausen et al., 1976) during a prescan delay which varied from 0.78 to 2.33 s. The residual water signal was attenuated using the subtraction method described by Marion et al. (1989) prior to data processing. If necessary, baseline correction was performed using a procedure analogous to FLATT (Güntert and Wüthrich, 1992).

The two-dimensional ^1H-^1H NMR experiments DQF-COSY (Piantini et al., 1982; Rance et al., 1983), TOCSY (Braunschweiler and Ernst, 1983; Bax and Davis, 1985a) and NOESY (Jeener et al., 1979; Macura et al., 1981) were recorded on a H_2O solution (with 10% D_2O) at 285, 295 and 303 K and on a D_2O solution at 303 K. ^1H-^{13}C correlated HSQC (Bodenhausen and Ruben, 1980), HMQC-COSY (Wagner and Brühwiler, 1986), and HSQC-TOCSY (Kessler et al., 1990; Norwood et al., 1990) spectra were obtained at 303 K using a D_2O solution.

TOCSY experiments were recorded with mixing times from 60 to 66 ms using a DIPSI-2 (Shaka et al., 1988) spin-lock pulse of 7.9–8.6 kHz in combination with two z-filters (Sørensen et al., 1984; Rance, 1987). The NOESY spectra obtained from H_2O solutions were recorded with mixing times of 150 ms (285 K) or 170 ms (295 and 303 K), while the mixing time used for the NOESY spectrum obtained from a D_2O solution was only 100 ms (at 303 K) in order to favour the intraresidual correlations between the β-protons and the adjacent ring protons of the aromatic residues. A 180° composite pulse was placed in the middle of the mixing period in all NOESY experiments. The ^1H 2D spectra consisted of 556 to 1024 t_1 data points and 4096 t_2 data points, corresponding to acquisition times between 15 and 27 h. The sweep width was 7353 Hz in both dimensions.

After zerofilling and Fourier transformation, the digital

Abbreviations: BPTI, bovine pancreatic trypsin inhibitor; α3(VI), 7–64 fragment of the 76-residue C5 Kunitz domain from the α3-chain of human type VI collagen; TPPI, time-proportional phase increment; DANTE, delays alternating with nutation for tailored excitation; DIPSI, decoupling in the presence of scalar interactions; DQF, double-quantum filtered; COSY, two-dimensional correlated spectroscopy; TOCSY, total correlation spectroscopy; NOE, nuclear Overhauser enhancement; NOESY, NOE correlated spectroscopy; HSQC, heteronuclear single-quantum coherence; HMQC, heteronuclear multiple-quantum coherence; 2D, two-dimensional; FID, free induction decay; ppm, parts per million; $d_{\alpha N}(i,j)$, distance and corresponding NOE connectivity between the H^α proton on residue i and the NH proton on residue j; $d_{NN}(i,j)$, $d_{\alpha N} = d_{\alpha N}(i,i+1)$, $d_{NN} = d_{NN}(i,i+1)$, $d_{\beta N} = d_{\beta N}(i,i+1)$, and $d_{\alpha\beta}(i,i+3)$ are defined accordingly; J_{NHH^α}, three-bond coupling between the α proton and the amide proton; C5, the 76-residue C5 Kunitz domain from the α3-chain of human type VI collagen; APPI, Alzheimer precursor protein inhibitor domain; Toxin I, dendrotoxin I from the venom of *Dendroaspis polylepis polylepis*; ShPI, Kunitz-type proteinase inhibitor from the Carribean sea anemone *Stichodactyla helianthus*; Toxin K, dendrotoxin K from the venom of *Dendroaspis polylepis polylepis*.

resolution of the ^1H 2D spectra was 3.6 Hz/point and 7.2 Hz/point in the F_2 and F_1 dimensions, respectively. The window functions used for resolution enhancement in the NOESY and TOCSY spectra were a Gaussian line-broadening function of −15 Hz and a scaling factor of 0.15 in the t_2 dimension, and a squared sine-bell function shifted 70° in the t_1 dimension. In the DQF-COSY spectra a combination of a sine-bell function and a squared cosine-bell function was used in both dimensions.

The J_{NHH^α} coupling constants were determined from a nonlinear least-squares fit of the expression for the discrete Fourier transformation (Abildgaard et al., 1988) to F_2 slices through the NH-H^α DQF-COSY cross peaks.

Discrimination between slow and fast exchanging amide protons was achieved by recording a TOCSY spectrum 24 to 41 h after dissolving the protein in 99.96% D_2O, and defining the amide protons still giving rise to cross peaks as slowly exchanging.

The heteronuclear ^1H-^{13}C experiments were recorded analogously to those used in a ^{13}C study of B9(Asp) insulin (Kristensen and Led, 1995). A mixing time of 40 ms was used in the HSQC-TOCSY experiments. The heteronuclear 2D spectra consisted of 256 to 421 t_1 data points and 4096 t_2 data points, corresponding to total acquisition times between 45 and 90 h. The sweep width was 10 000 Hz in both dimensions. The digital resolution of the HSQC and HSQC-TOCSY spectra was 4.9 Hz/point and 19.5 Hz/point in the F_2 and F_1 dimensions, respectively. A Gaussian line-broadening window function was used in the t_2 dimension and a sine-bell function shifted 70°, combined with a trapezoidal filtering function, in the t_1 dimension. The digital resolution of the HMQC-COSY spectra was 2.4 Hz/point and 19.5 Hz/point in the F_2 and F_1 dimensions, respectively. The data in the t_2 dimension were multiplied by a convolution difference function, combined with a squared cosine-bell function. In the t_1 dimension the applied window function was similar to that used for the HSQC and HSQC-TOCSY spectra.

To aid the identification of exchange cross peaks in the NOESY and TOCSY spectra, a two-dimensional exchange spectrum (sequence D of Fejzo et al., 1991) with a mixing time of 120 ms was recorded on the H_2O solution. The spectrum consisted of 512 t_1 data points and 4096 t_2 data points. The longitudinal relaxation delay, τ^n, was twice the length of a single 90° pulse. The B_1 field was 10.8 kHz. Data processing was analogous to that used for the NOESY and TOCSY spectra.

In order to determine the exchange rate between the two conformations of α3(VI), a series of NOESY spectra was recorded on the H_2O solution with mixing times of 10, 20, 30, 50, 80, 100, 150, 200, 300 and 400 ms. These NOESY experiments all consisted of 512 FIDs, each represented by 4096 t_2 data points. The total acquisition time for each NOESY spectrum in this series was 12 h.

For $Tyr^{22(28)}$, NH signal intensities used for the determination of the inter-conformational exchange rate were evaluated from slices through the exchange cross peaks in the NOESY spectrum. Thus, the relative intensities were obtained by a nonlinear least-squares fit of the expression for the discrete Fourier transformation (Abildgaard et al., 1988) to the F_2 slices that correspond to the frequencies of the major and minor conformation, respectively. The intensities of exchange peaks involving $Ala^{31(37)}$ NH, $Trp^{21(27)}$ H^α and $Gln^{48(54)}$ $H^{\beta 2}$ were obtained using an in-house written integration routine (S.M. Kristensen, unpublished results). The exchange rates were extracted from the resulting intensities by a nonlinear least-squares fit using an exchange model based on the modified Bloch equations for exchange between n sites (Schotland and Leigh, 1983; Gesmar and Led, 1986) with n = 2. The program MT (Nielsen, 1993) was used for fitting.

Results

Sequence-specific assignment

A nearly complete assignment of the ^1H and ^{13}C resonances was obtained by an analysis of ^1H-^1H spectra as outlined by Wüthrich (1986), and by examination of heteronuclear ^1H-^{13}C spectra. The quality of the ^1H-^1H spectra used in the assignment is illustrated in Fig. 1, which shows that the ^1H resonances of α3(VI) are characterized by good dispersion, as expected for a globular β-sheet protein. The ^1H-^{13}C HSQC, HSQC-TOCSY and especially the HMQC-COSY spectra were valuable not only for the assignment of the ^{13}C resonances but also for the assignment of the ^1H resonances, in particular the aromatic ring protons (vide infra). Only the spin system of $Cys^{14(20)}$ was not observed at 303 K, but could be identified at 285 K.

The assignment of the ^{13}C spectrum was based on preliminary ^1H assignments and the heteronuclear ^1H-^{13}C spectra, using the principles outlined by Kristensen and Led (1995). The problem of near-degeneracy in the ^1H dimension was overcome by the observation of relayed correlations and/or comparison between the measured and random-coil ^{13}C chemical shifts (Wüthrich, 1976; Howarth and Lilley, 1978).

Assignment of the aromatic ring systems by 2D ^1H-^{13}C NMR

A major problem in the assignment of ^1H resonances in proteins by 2D ^1H-^1H NMR is the assignment of the aromatic ring systems. This is primarily due to the limited dispersion of aromatic ^1H resonances. At the same time, the assignment of the aromatic ring systems is important for the determination of 3D protein structures by NMR, since these ring systems are often involved in hydrophobic interactions that determine the global fold of the protein.

The aromatic region of the HMQC-COSY spectrum is

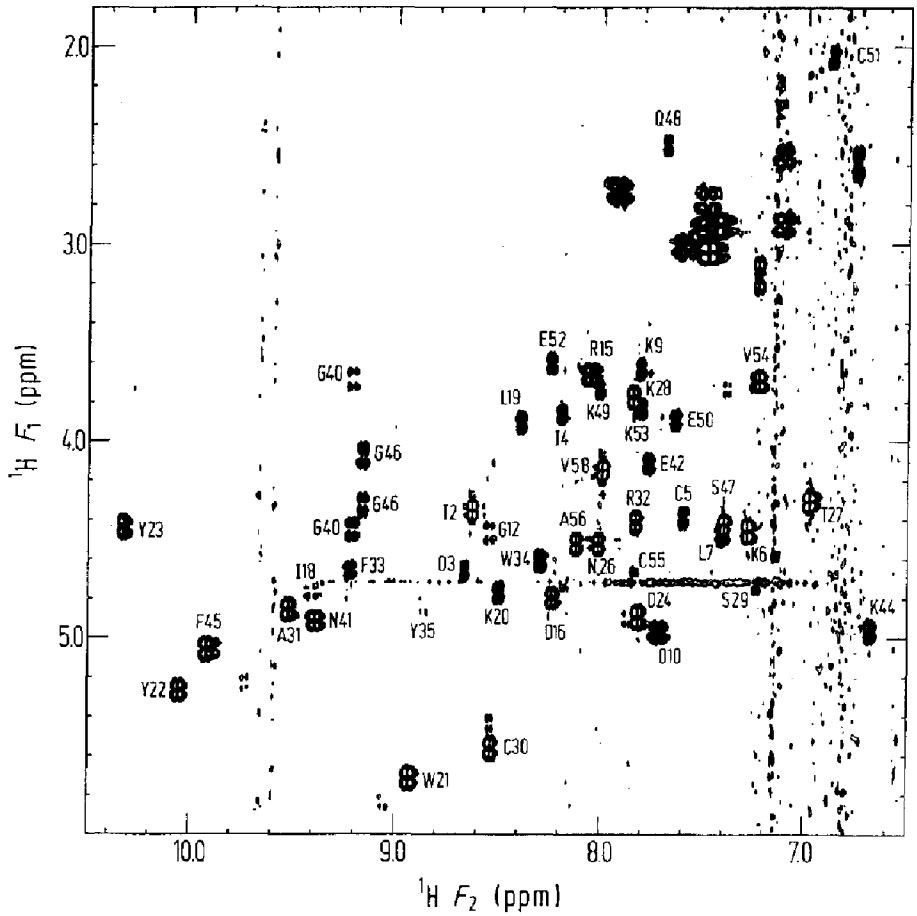

Fig. 1. The fingerprint region of the DQF-COSY spectrum of α3(VI) in H_2O (2 mM, pH 2.9, 303 K), showing primarily the correlations between the amide and H^{α} protons.

shown in Fig. 2a. The larger dispersion of the ^{13}C resonances in aromatic ring systems compared to the ^1H resonances makes the assignment of the tryptophan 7H-7C and tyrosine 3,5H-3,5C correlations straightforward. Since α3(VI) contains only three tyrosines, the observation of four signals in the spectral region containing the tyrosine 3,5H-3,5C correlations immediately suggests that the ring flipping of one of the tyrosine rings is hindered. The assignment of the 2,6H-2,6C correlations from the two tyrosines with fast ring flipping follows directly from the observation of relayed correlations (Fig. 2a). Also, the assignment of the tryptophan 6H, 5H and 4H protons (and the corresponding carbons) can be done on the basis of relayed correlations starting at the 7H-7C correlation (Fig. 2a).

The assignment of the remaining part of the tryptophan ring system, i.e., the N1H and the 2H protons, can be obtained on the basis of the strong NOEs from the 7H and 2H protons to the N1H proton and the characteristic correlation between the N1H and the 2H protons in a ^1H-^1H COSY spectrum. The aromatic rings of phenylalanine residues are more difficult to assign, due to the almost identical chemical shifts of the 2,6H and 3,5H protons and the 2,6C and 3,5C carbons (Wüthrich, 1976, 1986). However, by combining the HSQC, HSQC-TOCSY and HMQC-COSY spectra it is still possible to get a complete ^1H and ^{13}C assignment of the phenylalanine rings, as shown in the HMQC-COSY spectrum in Fig. 2a. This spectrum contains only two unassigned signals after the assignment of the phenylalanine ring systems. These signals can, therefore, be assigned to the 2H-2C and 6H-6C correlations from the tyrosine ring with slow ring flipping.

Finally, the assignment of the aromatic ring systems to specific residues was made on the basis of NOEs from the β-protons to the nearest ring protons (Wüthrich, 1986). From this assignment it follows that the tyrosine ring with slow ring flipping belongs to $Tyr^{35(41)}$. In BPTI, Tyr^{35} also shows hindered ring flipping (Wagner et al., 1975).

Further applications of 2D ^1H-^{13}C NMR

The importance of employing ^1H-^{13}C spectra in the ^1H assignment is further demonstrated by the identification of two mistakenly inverted assignments in the independent NMR study of the complete C5 domain (Zweckstetter et al., 1996). In that study, the chemical shifts of $Ser^{29(35)}$ H^{α} and H^{β} were reported to be 3.69 ppm and 4.72

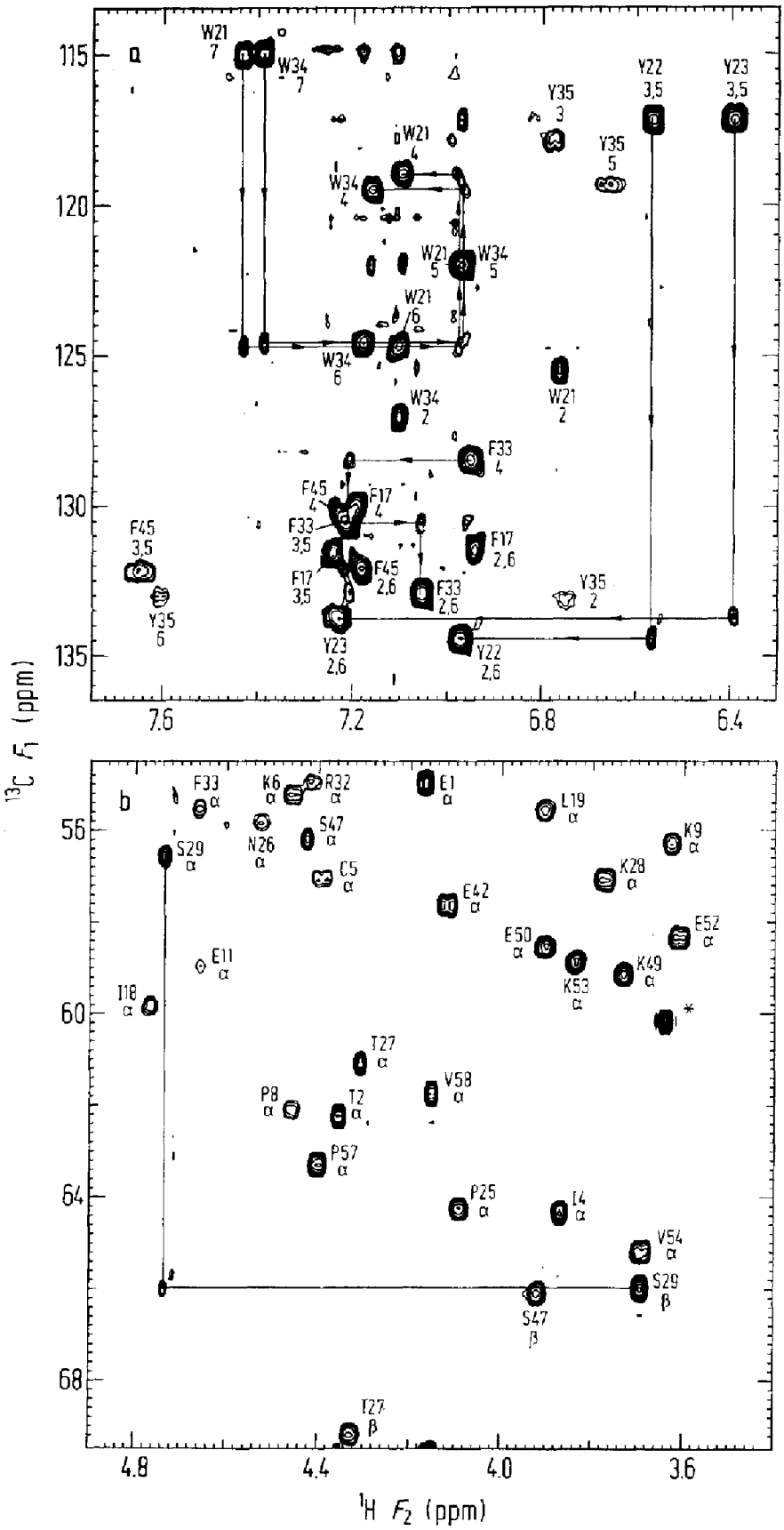

Fig. 2. Excerpts from the HMQC-COSY spectrum of α3(VI) (in D_2O, 2 mM, pD 2.9, 303 K), showing (a) the aromatic region and (b) the aliphatic region containing correlations from serines. The signal marked with an asterisk in (b) is from a small amount of ethanol.

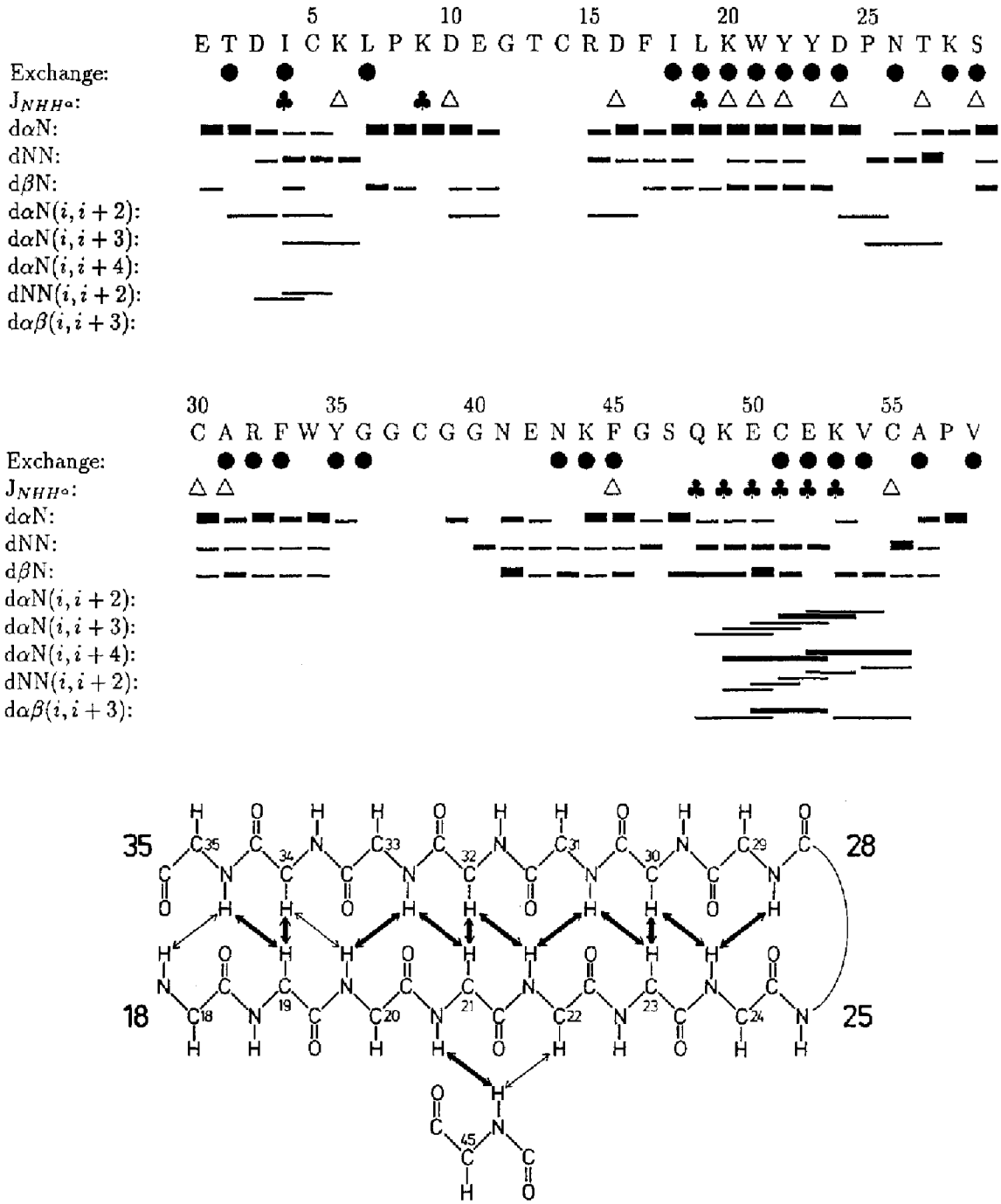

Fig. 3. Sequential, medium-range and long-range NOE connectivities used for the determination of the secondary structure. For proline residues the connectivities to the δ-protons are shown. The intensities of the NOE connectivities are indicated by the thickness of the bars/arrows. The NOEs were obtained from a NOESY spectrum of α3(VI) in H_2O, recorded with a mixing time of 170 ms. Backbone amide protons exchanging slowly with deuterons in D_2O are indicated with filled circles (●). Triangles (△) and clubs (♣) indicate J_{NHH^α} coupling constants that exceed 8 Hz or are smaller than 6 Hz by at least one standard deviation, respectively.

ppm, respectively. In contrast, the opposite assignment, that is 4.73 ppm for H^α and 3.69 ppm for H^β, is obtained in the present study using an assignment procedure supported by the ^1H-^{13}C correlations. It seems unlikely that the different pH used in the two studies (2.9 in the present study and 6.2 in the study by Zweckstetter et al.) is the cause of this discrepancy, since the chemical shifts of aliphatic protons are rather insensitive to changes in pH. The spectral region of the HMQC-COSY spectrum containing the correlations from the serine residues is shown in Fig. 2b. The β-strand chemical shifts of serine C^α and C^β are below 58.2 ppm and above 63.2 ppm, respectively (Spera and Bax, 1991). Inspection of Fig. 2b immediately reveals direct correlations at 3.69,66.0 ppm and 4.73,56.5

ppm and a relayed correlation at 4.73,66.0 ppm, strongly supporting the assignment presented here.

Other differences between the present study and that of Zweckstetter et al. (1996) are observed for $Leu^{7(13)}$ H^{β}/H^{γ}, $Lys^{44(50)}$ H^{γ}/H^{δ} and $Ser^{47(53)}$ $H^{\beta 2}$. Especially the case of $Ser^{47(53)}$ $H^{\beta 2}$ is intriguing: in the present work, only one β-methylene resonance is observed at 3.92 ppm, whereas Zweckstetter et al. observed two resonances ($H^{\beta 1}$ at 3.93 ppm and $H^{\beta 2}$ at 3.66 ppm).

In a 2D ^1H-^1H TOCSY spectrum obtained at 303 K we do in fact observe correlations at 3.73 ppm and the NH (7.40 ppm) and H^{α} (4.42 ppm) frequencies of $Ser^{47(53)}$. However, the proton resonating at 3.73 ppm is not $Ser^{47(53)}$ $H^{\beta 2}$, but $Ser^{47(53)}$ H^{α} in the minor conformation (vide infra) of α3(VI). This rather surprising conclusion is based on several observations. First, the lack of correlations at 3.73 and 3.92 ppm in the ^1H-^1H DQF-COSY spectrum, and at 3.73 and 66.1 ppm (the latter frequency being that of $Ser^{47(53)}$ C^{β}) in the ^1H-^{13}C HMQC-COSY spectrum (Fig. 2b) excludes $Ser^{47(53)}$ $H^{\beta 2}$ as the proton resonating at 3.73 ppm. Second, the observation of a weak correlation at 3.73 and 7.39 ppm in the DQF-COSY spectrum (Fig. 1) suggests that the proton resonating at 3.73 ppm is an H^{α} proton in a minor conformation, and, accordingly, that the TOCSY correlations at 3.73 ppm and the frequencies of $Ser^{47(53)}$ H^{α} and NH are due to exchange between two conformations.

The sequential assignments were made on the basis of a series of 2D NOESY spectra recorded at different temperatures, to allow discrimination of overlapping NH resonances. All sequential NOEs are indicated in Fig. 3. The ^1H and ^{13}C chemical shifts are tabulated in the Supplementary Material.

Secondary structure

The specific medium- (α-helix and turns) and long-range NOE patterns (β-sheet), the slowly exchanging amide protons, and the $J_{NHH^{\alpha}}$ coupling constants, all of which are summarized in Fig. 3, indicate that the principal secondary structure elements of α3(VI) are a central two-stranded β-sheet and a C-terminal α-helix. More specific, numerous intense $d_{\alpha N}$ connectivities, a series of $J_{NHH^{\alpha}}$ coupling constants ≥ 8 Hz, and a corresponding pattern of slowly exchanging amide hydrogens found in the central part of the molecule are all in accordance with a β-sheet structure. This is further supported by the observation of several long-range backbone NOEs in this region. Thus, the residues from $Ile^{18(24)}$ to $Tyr^{35(41)}$ form a two-stranded antiparallel β-sheet with one strand spanning residues 18(24) to 25(31) and the other spanning residues 29(35) to 35(41). In addition to the two major strands, $Phe^{45(51)}$ associates to the β-sheet to form a small third strand. The NOEs and coupling constants found for the residues from 25(31) to 28(34) indicate that these residues adopt a type-I turn conformation.

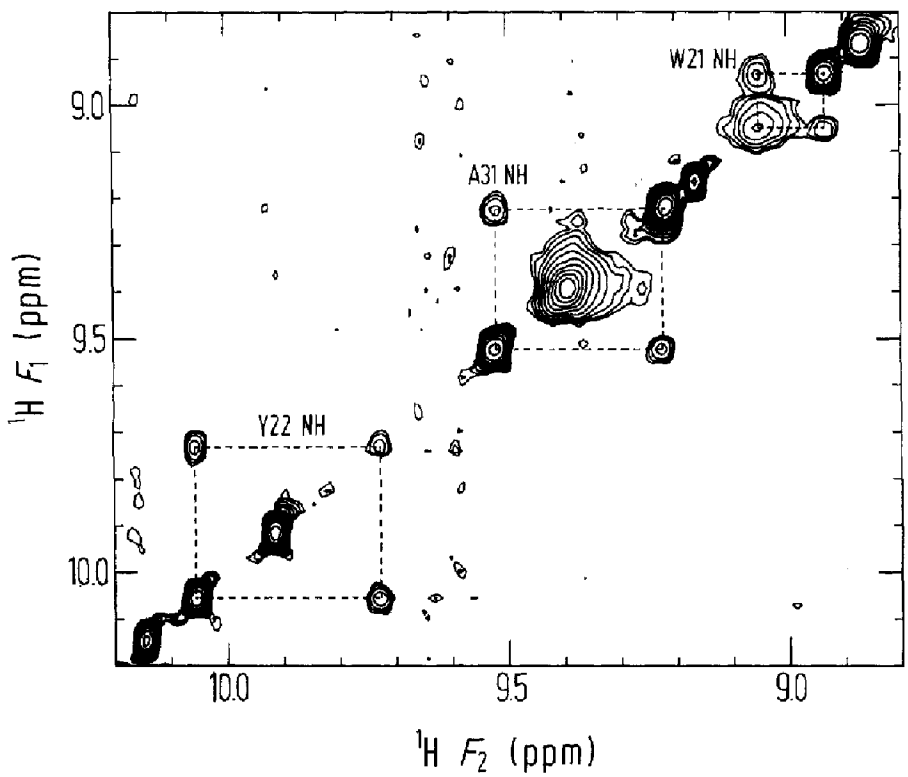

Fig. 4. Excerpt from the TOCSY spectrum of α3(VI) in H_2O (2 mM, pH 2.9, 303 K, mixing time 66 ms), showing exchange cross peaks between the major and minor conformations of three backbone amide protons. Only positive contour levels are shown.

TABLE 1
CHEMICAL SHIFT DIFFERENCES[a] BETWEEN THE ^{1}H RESONANCES OF THE MINOR AND MAJOR CONFORMATIONS OF α3(VI)

Residue	NH	αCH	βCH	Others
Leu$^{19(25)}$	−0.07	−0.18	−0.04, −0.09	γCH −0.12; δCH$_3$ −0.18, 0.07
Lys$^{20(26)}$	−0.29			
Trp$^{21(27)}$	0.13	0.12	0.12	C2H −0.19; C7H −0.07; C6H 0.02; C5H −0.11; C4H 0.43
Tyr$^{22(28)}$	0.32			
Asp$^{24(30)}$	0.07		0.03, −0.05	
Asn$^{26(32)}$	−0.10		0.03, 0.06	
Cys$^{30(36)}$		−0.14	−0.74/−0.20[b]	
Ala$^{31(37)}$	−0.30			
Arg$^{32(38)}$	0.27	−0.18		γCH$_2$ 0.97, 0.81
Trp$^{34(40)}$				C2H −0.04; N1H −0.02
Tyr$^{35(41)}$	−0.08			
Ser$^{47(53)}$	−0.01	−0.69		
Gln$^{48(54)}$	−0.14		1.53	δNH 0.11
Glu$^{50(56)}$	0.06			
Glu$^{52(58)}$	−0.06			

[a] At 303 K and pH 2.9. Chemical shift differences are defined as $\Delta\delta = \delta_m - \delta_M$. Only protons with chemical shift values that are different in the major and the minor conformation are listed. Stereospecific assignments of β-methylene protons are indicated by underlined Δδ values. The H$^{\beta 2}$ protons are listed first.
[b] Cannot be assigned unambiguously to H$^{\beta 2}$ or H$^{\beta 3}$.

The medium-range NOEs and coupling constants ≤ 6 Hz observed in the C-terminal part of the molecule clearly indicate a regular α-helix starting at Gln$^{48(54)}$, although there are some difficulties in defining the C-terminal residue. Thus, the fast exchange of Cys$^{55(61)}$ NH and the $J_{NH^{\alpha}}$ coupling constants of Cys$^{55(61)}$ and Ala$^{56(62)}$ indicate that the C-terminal residue is Val$^{54(60)}$, while the medium-range NOEs suggest that Ala$^{56(62)}$ is the C-terminal residue. The observation of two $d_{\alpha N(i,i+2)}$ connectivities, in addition to a $d_{\alpha N(i,i+3)}$ and two $d_{NN(i,i+2)}$ in the N-terminal part of the molecule, suggest that residues 2(8) to 7(13) adopt an irregular 3_{10}-helical conformation.

Experimental evidence for two exchanging protein conformations

Figure 4 shows part of the NH-NH region of the TOCSY spectrum of α3(VI) at 303 K. Three cross peaks are observed in this region, all of which are caused by magnetization transfer due to exchange, as shown below.

In general, three types of magnetization transfer can generate cross peaks in a TOCSY spectrum. First, the magnetization can be transferred by scalar coupling within the J-coupling network of spin systems (homonuclear Hartmann–Hahn transfer) (Braunschweiler and Ernst, 1983; Bax and Davis, 1985a). Second, as in the NOESY experiment, exchange processes can give rise to magnetization transfer which results in cross peaks (Hennig and Limbach, 1982; Bleich and Wilde, 1984). Finally, ROESY cross peaks can be generated due to dipolar cross-relaxation in the rotating frame (Bax and Davis, 1985b).

In contrast to the phase of the exchange and J-coupling cross peaks, the ROESY cross peaks are 180° out of phase relative to the diagonal peaks. Therefore, the cross peaks shown in Fig. 4 cannot be caused by ROESY effects. Furthermore, these cross peaks involve only backbone amide protons, as no other protons have resonances at these frequencies (Table 1 of the Supplementary Material). This, together with the fact that J-couplings are not observed between two backbone amide protons, excludes the possibility that the observed cross peaks are caused by J-coupling. Therefore, the cross peaks in Fig. 4 are caused by magnetization transfer between two exchanging protein conformations, where the amide protons change from one environment to another through structural isomerization. The intensities of the diagonal signals show that the two protein conformations are not equally populated, i.e. there is a major and a minor conformation.

In addition to the protons shown in Fig. 4, a number of other protons have different chemical shifts in the major and minor conformations. Table 1 lists the chemical shift differences for these protons in the minor and major conformations. In most cases the chemical shift difference between the two conformations is small and the direct exchange peaks are, therefore, too close to the diagonal to be observed. In these cases the identification of protons with different chemical shifts in the two conformations was based on the observation of rectangular TOCSY cross-peak patterns (Feng and Roder, 1988) and/or observation of cross peaks with the same phase as the diagonal in a two-dimensional exchange spectrum.

Determination of the rate of exchange between the two conformations of α3(VI)

The rate of magnetization transfer between two sites

(M,m) due to cross-relaxation, R_{Mm}, and slow chemical exchange, k_{Mm}, can readily be determined by recording a series of NOESY experiments with different mixing times (Jeener et al., 1979; Kumar et al., 1981). An analysis of the dependency of the diagonal and cross-peak intensities on the mixing time, using an appropriate exchange model based on the modified Bloch equations, will subsequently result in determination of the exchange rates. However, due to the formal similarity between cross-relaxation and chemical exchange, it is not possible to distinguish between R_{Mm} and k_{Mm}. Therefore, it has to be assumed that one of the magnetization transfer processes can be neglected in order to determine the rate of the other process unambiguously. In the present application it is implicitly assumed that $R_{Mm}=0$; that is, no cross-relaxation occurs between the two protein conformations.

The amide proton of $Tyr^{22(28)}$ represents an ideal probe for measuring the exchange rate between the two conformations of α3(VI), for two reasons. First, as shown in Fig. 4, the chemical shift difference between the major and minor form is relatively large for $Tyr^{22(28)}$ NH, thus giving rise to exchange cross peaks that are well separated from the diagonal. Second, no spectral overlap is observed for the major and minor form of $Tyr^{22(28)}$ NH, which allows an unambiguous determination of the intensities of the diagonal peaks. On the basis of a backward exponential extrapolation of the intensities of the $Tyr^{22(28)}$ NH diagonal peaks to a mixing time of zero, the population of the minor conformation was found to be 6.4 ± 0.2% at 303 K.

The exchange rate was determined from a least-squares fit to the intensities of the diagonal and exchange cross peaks of $Tyr^{22(28)}$ NH as well as $Trp^{21(27)}$ H^{α}, $Ala^{31(37)}$ NH, and $Gln^{48(54)}$ $H^{\beta 2}$ (only the diagonal peak of the major conformation could be used for the latter two), using an exchange model that describes a two-state equilibrium between the major conformation, M, and the minor conformation, m (Eq. 1).

$$M \underset{k_m}{\overset{k_M}{\rightleftharpoons}} m \qquad (1)$$

The exchange rate constants, k_M, obtained from these four protons were 1.07, 0.98, 1.46 and 0.98 s^{-1}, respectively. The relatively large value of 1.46 s^{-1} measured from $Ala^{31(37)}$ NH suggests that this value is somewhat inaccurate and might be a consequence of using only the intensity of the diagonal peak of the major conformation for the determination. However, excluding the intensity of the diagonal peak of the minor conformation in the cases of $Tyr^{22(28)}$ NH and $Trp^{21(27)}$ H^{α} only changed the exchange rate constants determined from these protons insignificantly. Moreover, examination of the ^1H assignment of α3(VI) revealed that $Phe^{33(39)}$ NH resonates at the same frequency as $Ala^{31(37)}$ NH in the minor conformation. It therefore seems likely that the intensity of the exchange peak of $Ala^{31(37)}$ NH, in addition to magnetization transferred through exchange, also includes magnetization transferred from $Phe^{33(39)}$ NH to $Ala^{31(37)}$ NH, thus leading to an overestimated k_M value. The three k_M values obtained from $Tyr^{22(28)}$ NH, $Trp^{21(27)}$ H^{α}, and $Gln^{48(54)}$ $H^{\beta 2}$ correspond to an average value of 1.01 ± 0.05 s^{-1}.

Discussion

The sequential proton assignment of α3(VI) is virtually complete, the exceptions being $Thr^{13(19)}$ NH and H^{α} and the $Cys^{38(44)}$ β-protons. The missing assignment of these protons is probably a consequence of exchange broadening caused by structural isomerization of the $Cys^{14(20)}$-$Cys^{38(44)}$ disulfide bond (vide infra). The striking similarity of the secondary structure elements of α3(VI) and BPTI, together with the fact that 33% of the amino acids are identical in the two proteins, strongly suggests that their global folds are very similar. Subsequently, this suggestion has been confirmed by a determination of the 3D solution structure of α3(VI) using the program X-PLOR (Brünger, 1992; to be published), and also by the independently determined solution structure of the complete C5 domain (Zweckstetter et al., 1996) and the crystal structure of α3(VI) (Arnoux et al., 1995). The similarity of the 3D structures of α3(VI) and other Kunitz-domain proteins (Wagner et al., 1987; Heald et al., 1991; Antuch et al., 1993; Berndt et al., 1993; Foray et al., 1993; Zweckstetter et al., 1996) is also illustrated by the observation of a

TABLE 2
UNUSUAL H^{α} CHEMICAL SHIFT VALUES (ppm) CONSERVED IN KUNITZ-TYPE PROTEINS[a]

Residue	α3(VI)	C5	BPTI	APPI	Toxin I	ShPI	Toxin K
21(27)	5.71	5.73	5.68	5.54	5.83	5.64	5.86
22(28)	5.27	5.28	5.26	5.30	5.14	5.64	5.35
30(36)	5.58	5.56	5.62	5.70	5.42	4.93	5.47
45(51)	5.06	5.06	5.13	5.21	4.97	5.09	5.01
48(54)	2.50	2.51	3.14	2.54	3.10	2.99	3.05
51(57)	2.05	2.08	1.70	2.20	1.90	2.23	2.00

[a] Chemical shift values from: C5: Zweckstetter et al. (1996); BPTI: Wagner et al. (1987); APPI: Heald et al. (1991); Toxin I: Foray et al. (1993); ShPI: Antuch et al. (1993); Toxin K: Berndt et al. (1993).

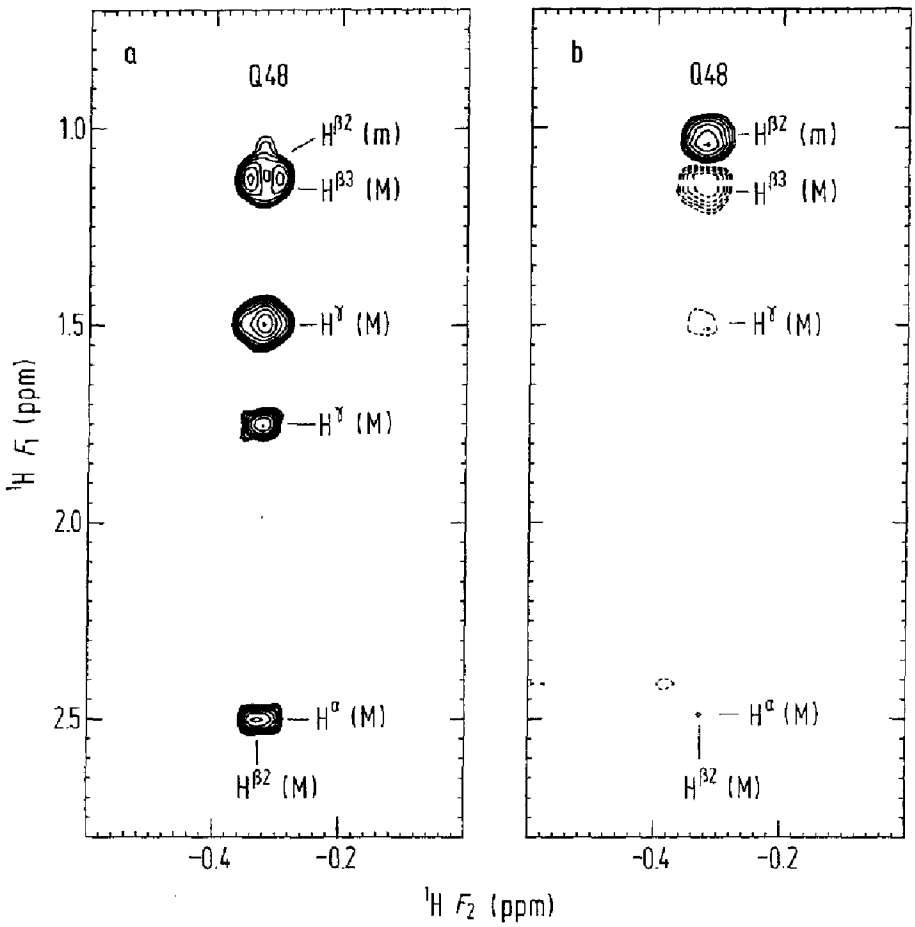

Fig. 5. Excerpt from (a) a TOCSY spectrum (mixing time 66 ms) and (b) an exchange spectrum using sequence D of Fejzo et al. (1991) (mixing time 120 ms) of α3(VI) in H_2O, showing correlations to the major conformation of Gln^{48} $H^{\beta 2}$. Negative contour levels are indicated by dashed lines.

number of unusual H^{α} chemical shift values, which are conserved in this family of proteins (Table 2). Noteworthy is also the observation of a highly upfield shifted NH resonance of $Gly^{37(43)}$ (4.46 ppm, see Table 1 of the Supplementary Material), similar to that found for Gly^{37} NH in BPTI (Tüchsen and Woodward, 1987). This suggests a similar interaction between the ring of $Tyr^{35(41)}$ and $Gly^{37(43)}$ NH in α3(VI) and BPTI.

Characterization of the two exchanging conformations of α3(VI)

A large number of protons with different chemical shifts in exchanging conformations were also observed in the study of the complete C5 domain by Zweckstetter et al. (1996). In this study the residues existing in multiple conformations were divided into three patches, (i) one located in the central β-sheet; (ii) one consisting of the residues around the Cys^{20}-Cys^{44} disulfide bond; and finally (iii) one in the vicinity of the Cys^{11}-Cys^{61} disulfide bond. In the present study the residues found to exist in two exchanging conformations are all located in the vicinity of the central β-sheet and, therefore, correspond to the first patch defined by Zweckstetter et al. (1996). It was suggested by these authors that the origin of the different conformations observed for the residues in patches (ii) and (iii) could be an isomerization of the Cys^{20}-Cys^{44} and Cys^{11}-Cys^{61} disulfide bonds, respectively, whereas no interpretation was offered for the observation of multiple conformations in the central β-sheet. In the following, it will be shown that also in the case of α3(VI) an isomerization of the $Cys^{14(20)}$-$Cys^{38(44)}$ disulfide bond is likely, and that the origin of multiple conformations in the central β-sheet is a reorientation of the $Trp^{21(27)}$ ring.

Isomerization of the $Cys^{14(20)}$-$Cys^{38(44)}$ disulfide bond

Otting et al. (1993) found that exchange between two conformers with different chirality of the Cys^{14}-Cys^{38} disulfide bond occurs in wild-type BPTI and in the mutant BPTI(G36S). This conclusion was based on the observation of different chemical shifts for residues 12–18 and 34–40 in a major and minor conformation of BPTI(G36S), and on the presence of exchange cross peaks for nearly all of these residues in a difference spectrum of the [^{15}N,^1H]-two-spin-order exchange experiment (Wider et al., 1991).

In the case of α3(VI), only one set of chemical shifts is observed for residues 12(18) to 18(24) at a temperature of 303 K. Even so, there are several indications of $Cys^{14(20)}$-$Cys^{38(44)}$ disulfide bond isomerization. Thus, the signal of $Cys^{38(44)}$ NH broadens with increasing temperature in the temperature range from 285 to 303 K (data not shown). This strongly suggests that $Cys^{38(44)}$ NH is affected by conformational averaging. Furthermore, the fact that signals from $Cys^{14(20)}$ are observed only at 285 K agrees with a structural isomerization of the $Cys^{14(20)}$-$Cys^{38(44)}$ disulfide bond. Finally, the observation of only one $Cys^{38(44)}$ NH resonance at 285 K is consistent with a decreasing population of the minor conformation with decreasing temperature, as observed previously for Cys^{14}-Cys^{38} disulfide bond isomerization in BPTI (Otting et al., 1993).

Reorientation of the $Trp^{21(27)}$ ring

The observation of signals from a major and a minor conformation of the residues listed in Table 1 cannot be explained by the above-mentioned structural isomerization of the $Cys^{14(20)}$-$Cys^{38(44)}$ disulfide bond, for several reasons. First, with the exception of $Tyr^{35(41)}$, none of the residues in Table 1 are located in the vicinity of the $Cys^{14(20)}$-$Cys^{38(44)}$ disulfide bond, neither sequentially nor sterically. Second, no exchange line broadening similar to that found for $Cys^{38(44)}$ NH is observed for any of the residues in Table 1 in the temperature range from 285 to 303 K. Finally, in contrast to the temperature dependency of the $Cys^{14(20)}$-$Cys^{38(44)}$ disulfide bond isomerization in BPTI, the population of the minor conformation of α3(VI) increases with decreasing temperature (data not shown). This temperature dependency was also observed for the residues in the central β-sheet of the complete C5 domain (Zweckstetter et al., 1996).

Exchange cross peaks arising from the amide protons of Tyr^{22} and Ala^{31} and several Trp^{21} protons have been observed previously in an NMR study of the Kunitz-domain protein APPI (Heald et al., 1991). In the case of APPI, it was suggested that the presence of exchange NOEs from these residues might be a consequence of a dynamic reorientation of the Trp^{21} ring. In the 3D solution structure of APPI, the Trp^{21} ring was found to be positioned in the hydrophobic groove created between the β-sheet and the C-terminal α-helix (Heald et al., 1991). Furthermore, it was shown that the Trp^{21} ring is situated over the two hydrogen bonds in the β-sheet involving Tyr^{22} NH and Ala^{31} NH, thus affecting these amide protons by local anisotropic effects.

In the light of the observations made for APPI, it is intriguing that among the amide protons of α3(VI) the two with the largest difference between the major and minor chemical shift values are $Tyr^{22(28)}$ NH and $Ala^{31(37)}$ NH (Table 1). This, together with the observation of different chemical shift values for nearly all $Trp^{21(27)}$ protons, strongly suggests that the two exchanging conformations of α3(VI) differ in the orientation of the $Trp^{21(27)}$ ring.

Further evidence for this conclusion comes from the $Gln^{48(54)}$ $H^{\beta 2}$, $Ser^{47(53)}$ H^{α}, and $Arg^{32(38)}$ $H^{\gamma 1}$ and $H^{\gamma 2}$ protons. As shown in Fig. 5a, an exchange cross peak is observed for $Gln^{48(54)}$ $H^{\beta 2}$ at 303 K in the TOCSY spectrum at −0.48 ppm (major conformation) and 1.03 ppm (minor conformation), corresponding to a chemical shift differ-

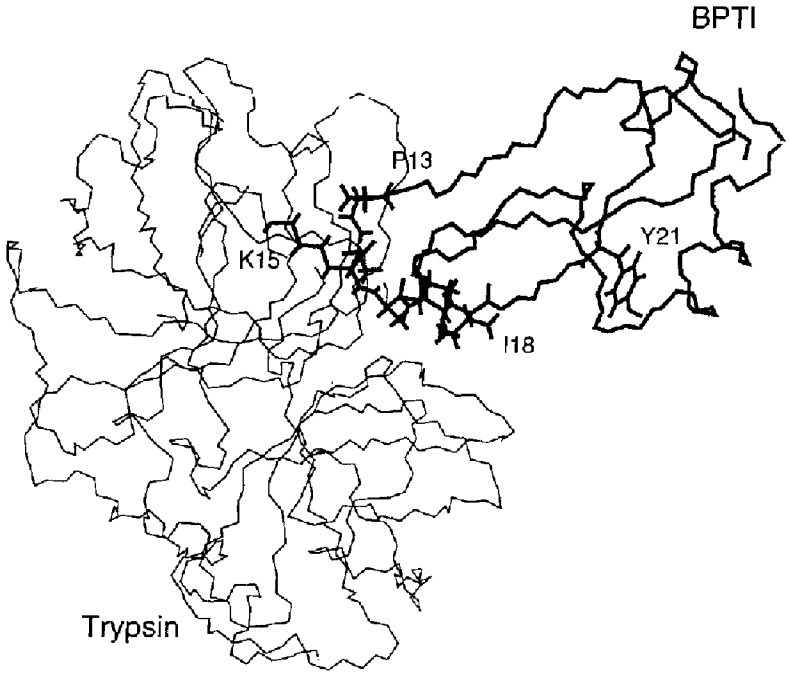

Fig. 6. Crystal structure of the trypsin/BPTI complex (PDB access code 2PTC, Marquart et al., 1983), showing the position of residue 21 relative to the binding loop composed of residues 13 to 18. The labelled residues are located in BPTI.

ence of 1.53 ppm. The identification of this cross peak as an exchange cross peak was based on two observations. First, the exchange rate k_M measured from this cross peak is 0.98 s^{-1}, which, within the experimental error, is identical to the values obtained from $Tyr^{22(28)}$ NH and $Trp^{21(27)}$ H^{α}. Second, in a 2D exchange spectrum (Fejzo et al., 1991) this cross peak has the same phase as the diagonal, whereas the corresponding TOCSY correlations are eliminated or have the opposite phase (Fig. 5b). The fact that cross peaks with a phase opposite to that of the diagonal peaks are observed in the exchange spectrum indicates that the condition $\omega\tau_c \gg 1$ is not fulfilled for α3(VI) at 303 K (Fejzo et al., 1991).

Heald et al. (1991) found a chemical shift value of –0.69 ppm for Glu^{48} $H^{\beta 2}$ in APPI and explained this unusually low value by a ring current effect from the Trp^{21} ring. It can be seen from the crystal structure of α3(VI) (Arnoux et al., 1995) that the low value of –0.48 ppm found for $Gln^{48(54)}$ $H^{\beta 2}$ in α3(VI) is due to a position of this proton similar to the position of Glu^{48} $H^{\beta 2}$ in APPI, i.e., directly above the $Trp^{21(27)}$ ring. The very large chemical shift difference (1.53 ppm) between the minor and major conformations of $Gln^{48(54)}$ $H^{\beta 2}$ is therefore most likely a consequence of a reorientation of the Trp^{21} ring.

$Ser^{47(53)}$ H^{α} and $Arg^{32(38)}$ $H^{\gamma 1}$ and $H^{\gamma 2}$ are all located less than 3.5 Å from the $Trp^{21(27)}$ ring in the crystal structure of α3(VI) (Arnoux et al., 1995). Therefore, further evidence for the reorientation of the $Trp^{21(27)}$ ring comes from the observation that these protons, like $Gln^{48(54)}$ $H^{\beta 2}$, have very different chemical shifts in the major and minor conformations (Table 1).

The fluorescence properties of the indole side chain of tryptophan makes fluorescence studies of α3(VI) seem natural in the context of a reorientation of the $Trp^{21(27)}$ ring. However, the fluorescence spectrum of α3(VI) is not sufficiently resolved to distinguish between $Trp^{21(27)}$ and $Trp^{34(40)}$. Consequently, fluorescence studies of the described reorientation of the $Trp^{21(27)}$ ring are not feasible. This further demonstrates the large potentiality of NMR to provide detailed information at the atomic level.

The most important residue for the trypsin inhibitory activity is residue 15, which has to be either lysine or arginine. This residue binds in the binding pocket of trypsin, where it forms a favorable salt linkage with the negatively charged Asp^{189} of trypsin, which is positioned at the bottom of the binding pocket. Subsequent to binding, the carbonyl carbon atom of residue 15 in the inhibitor is close to the OH oxygen of trypsin's reactive Ser^{195}, enabling a very slow cleavage of the 15–16 peptide bond. Also, the alanine in position 16 is important for the inhibitory activity of BPTI. Upon binding of BPTI, the small alanine side chain allows His^{57} of trypsin to move (with concomitant movements of Ser^{195} and Asp^{102}) to optimize hydrogen bonding distances. In contrast, an aspartate in position 16 of the inhibitor is able to form hydrogen bonds with the peptide group of His^{57} in trypsin and thereby prevents this residue from adjusting to the geometry necessary for bond cleavage (Dufton, 1985). The lack of inhibitory activity of α3(VI) towards trypsin can partly be explained by the aspartate in position 16(22) (Arnoux et al., 1995; Zweckstetter et al., 1996). Of importance is also the phenylalanine in position 17(23), which might introduce steric hindrance between the aromatic ring of $Phe^{17(23)}$ and Gln^{192} and Gly^{193} of trypsin (Arnoux et al., 1995).

Figure 6 shows the crystal structure of the trypsin/BPTI complex (Marquart et al., 1983). It is evident from this structure that residue 21 is relatively distant from the binding loop (residues 13 to 18). Accordingly, the similarity between the structures of α3(VI) and BPTI suggests that a reorientation of the $Trp^{21(27)}$ ring has little or no effect on the inhibitory activity. It should be noted, however, that further investigations, such as substitution of $Trp^{21(27)}$ with phenylalanine or tyrosine, are needed to clarify this point.

Conclusions

Taken together, the observations presented here show that a reorientation of the $Trp^{21(27)}$ ring is the origin of the multiple conformations in the central β-sheet observed for α3(VI), and most likely also of the multiple conformations of the central β-sheet in the complete C5 domain (Zweckstetter et al., 1996) and APPI (Heald et al., 1991). It seems likely that all Kunitz-domain proteins with a tryptophan in position 21 (referring to the sequence numbering of BPTI) will exist in a major and minor conformation, slowly exchanging on the NMR time scale. Examination of the crystal structure of the trypsin/BPTI complex suggests that a reorientation of the $Trp^{21(27)}$ ring has little or no effect on the inhibitory activity.

Acknowledgements

This work was supported by the Danish Technical Research Council, J. Nos 16-4963-1, 16-5028-1 and 9400446, the Danish Natural Science Research Council, J. No. 9400903, the Ministry of Industry, J. No. 85886, Julie Damms Studiefond, Direktør Ib Henriksens Fond and Novo Nordisk Fondet. We thank Dr. Georg Ole Sørensen for computational assistance.

References

Abildgaard, F., Gesmar, H. and Led, J.J. (1988) *J. Magn. Reson.*, **79**, 78–89.

Antuch, W., Berndt, K.D., Chávez, M.A., Delfin, J. and Wüthrich, K. (1993) *Eur. J. Biochem.*, **212**, 675–684.

Arnoux, B., Mérigeau, K., Saludjian, P., Norris, F., Norris, K., Bjørn, S., Olsen, O., Petersen, L. and Ducruix, A. (1995) *J. Mol. Biol.*, **246**, 609–617.

Bax, A. and Davis, D.G. (1985a) *J. Magn. Reson.*, **65**, 355–360.
Bax, A. and Davis, D.G. (1985b) *J. Magn. Reson.*, **64**, 533–535.
Berndt, K.D., Güntert, P. and Wüthrich, K. (1993) *J. Mol. Biol.*, **234**, 735–750.
Bleich, H. and Wilde, J. (1984) *J. Magn. Reson.*, **56**, 149–150.
Bodenhausen, G., Freeman, R. and Morris, G.A. (1976) *J. Magn. Reson.*, **23**, 171–175.
Bodenhausen, G. and Ruben, R.R. (1980) *Chem. Phys. Lett.*, **69**, 185–189.
Bodenhausen, G., Vold, R.L. and Vold, R.R. (1980) *J. Magn. Reson.*, **37**, 93–106.
Braunschweiler, L. and Ernst, R.R. (1983) *J. Magn. Reson.*, **53**, 521–528.
Brünger, A.T. (1992) *X-PLOR Manual*, Yale University, New Haven, CT, U.S.A.
Chu, M.-L., Zhang, R.-Z., Pan, T.-c., Stokes, D., Conway, D., Kuo, H.-J., Glanville, R., Mayer, U., Mann, K., Deutzmann, R. and Timpl, R. (1990) *EMBO J.*, **9**, 385–393.
Drobny, G., Pines, A., Sinton, S., Weitekamp, D.P. and Wemmer, D. (1979) *Faraday Div. Chem. Soc. Symp.*, **13**, 49–55.
Dufton, M.J. (1985) *Eur. J. Biochem.*, **153**, 647–654.
Fejzo, J., Westler, W.M., Macura, S. and Markley, J.L. (1991) *J. Magn. Reson.*, **92**, 20–29.
Feng, Y. and Roder, H. (1988) *J. Magn. Reson.*, **78**, 597–602.
Foray, M.-F., Lancelin, J.-M., Hollecker, M. and Marion, D. (1993) *Eur. J. Biochem.*, **211**, 813–820.
Gesmar, H. and Led, J.J. (1986) *J. Magn. Reson.*, **68**, 95–101.
Güntert, P. and Wüthrich, K. (1992) *J. Magn. Reson.*, **96**, 403–407.
Heald, S.L., Tilton Jr., R.F., Hammond, L.J., Lee, A., Bayney, R.M., Kamarck, M.E., Ramabhadran, T.V., Dreyer, R.N., Davis, G., Unterbeck, A. and Tamburini, P.P. (1991) *Biochemistry*, **30**, 10467–10478.
Hennig, J. and Limbach, H.H. (1982) *J. Magn. Reson.*, **49**, 322–328.
Howarth, O.W. and Lilley, D.M.J. (1978) *Prog. NMR Spectrosc.*, **12**, 1–40.
Jeener, J., Meier, B.H., Bachmann, P. and Ernst, R.R. (1979) *J. Chem. Phys.*, **71**, 4546–4553.
Kessler, H., Schmieder, P. and Bermel, W. (1990) *Biopolymers*, **30**, 465–475.
Kitaguchi, N., Takahashi, Y., Tokushima, Y., Shiojiri, S. and Ito, H. (1988) *Nature*, **331**, 530–532.
Kristensen, S.M. and Led, J.J. (1995) *Magn. Reson. Chem.*, **33**, 461–470.
Kumar, A., Wagner, G., Ernst, R.R. and Wüthrich, K. (1981) *J. Am. Chem. Soc.*, **103**, 3654–3658.
Macura, S., Huang, Y., Suter, D. and Ernst, R.R. (1981) *J. Magn. Reson.*, **43**, 259–281.
Marion, D. and Wüthrich, K. (1983) *Biochem. Biophys. Res. Commun.*, **113**, 967–974.
Marion, D., Ikura, M. and Bax, A. (1989) *J. Magn. Reson.*, **84**, 425–430.
Marquart, M., Walter, J., Deisenhofer, J., Bode, W. and Huber, R. (1983) *Acta Crystallogr.*, **B39**, 480–490.
Nielsen, P.F. (1993) Manual for Program MT, v. 2.0, University of Copenhagen, Copenhagen, Denmark.
Norwood, T.J., Boyd, J., Heritage, J.E., Soffe, N. and Campbell, I.D. (1990) *J. Magn. Reson.*, **87**, 488–501.
Otting, G., Liepinsh, E. and Wüthrich, K. (1993) *Biochemistry*, **32**, 3571–3582.
Piantini, U., Sørensen, O.W. and Ernst, R.R. (1982) *J. Am. Chem. Soc.*, **104**, 6800–6801.
Ponte, P., Gonzalez-DeWhitt, P., Schilling, J., Miller, J., Hsu, D., Greenberg, B., Davis, K., Wallace, W., Lieberburg, I., Fuller, F. and Cordell, B. (1988) *Nature*, **331**, 525–527.
Rance, M., Sørensen, O.W., Bodenhausen, G., Wagner, G., Ernst, R.R. and Wüthrich, K. (1983) *Biochem. Biophys. Res. Commun.*, **117**, 479–485.
Rance, M. (1987) *J. Magn. Reson.*, **74**, 557–564.
Redfield, A.G. and Kunz, S.D. (1975) *J. Magn. Reson.*, **19**, 250–254.
Schotland, J. and Leigh, J.S. (1983) *J. Magn. Reson.*, **51**, 48–55.
Shaka, A.J., Lee, C.J. and Pines, A. (1988) *J. Magn. Reson.*, **77**, 274–293.
Sørensen, O.W., Rance, M. and Ernst, R.R. (1984) *J. Magn. Reson.*, **56**, 527–539.
Spera, S. and Bax, A. (1991) *J. Am. Chem. Soc.*, **113**, 5490–5492.
Tanzi, R.E., McClatchey, A.I., Lamperti, E.D., Villa-Komaroff, L., Gusella, J.F. and Neve, R.L. (1988) *Nature*, **331**, 528–530.
Tüchsen, E. and Woodward, C. (1987) *Biochemistry*, **26**, 1918–1925.
Wagner, G., DeMarco, A. and Wüthrich, K. (1975) *J. Magn. Reson.*, **20**, 565–569.
Wagner, G. and Brühwiler, D. (1986) *Biochemistry*, **25**, 5839–5843.
Wagner, G., Braun, W., Havel, T.F., Schaumann, T., Gō, N. and Wüthrich, K. (1987) *J. Mol. Biol.*, **196**, 611–639.
Wider, G., Neri, D. and Wüthrich, K. (1991) *J. Biomol. NMR*, **1**, 93–98.
Williams, R.J.P. (1989) *Eur. J. Biochem.*, **183**, 479–497.
Wodak, S.J., Crombrugghe, M.D. and Janin, J. (1987) *Prog. Biophys. Mol. Biol.*, **49**, 29–63.
Wüthrich, K. (1976) *NMR in Biological Research: Peptides and Proteins*, North Holland, Amsterdam, The Netherlands.
Wüthrich, K. (1986) *NMR of Proteins and Nucleic Acids*, Wiley, New York, NY, U.S.A.
Zweckstetter, M., Czisch, M., Mayer, U., Chu, M.-L., Zinth, W., Timpl, R. and Holak, T.A. (1996) *Structure*, **4**, 195–209.